

# A new stand-alone QEXAFS data acquisition system for *in situ* studies

Jan Stötzel,\* Dirk Lützenkirchen-Hecht and Ronald Frahm

Fachbereich C – Physik, Universität Wuppertal, Gausstrasse 20, 42097 Wuppertal, Germany.  
E-mail: j.stoetzel@uni-wuppertal.de

To meet the demands of the QEXAFS (quick-scanning extended X-ray absorption fine structure) technique for a fast, user-friendly and flexible data acquisition a new stand-alone system with new software exploiting a multi-functional USB board was designed. The chosen approach allows the scanning of several analogue and digital data sources with up to 500000 samples each second over hours storable in binary or ASCII format without any dead-time. At the same time it is possible to visualize the acquired data instantaneously which provides a maximum of interactivity during the running experiment and also optimal conditions to select the best suited beamline and detector settings prior to each measurement. Furthermore, the QEXAFS monochromator and typically three current amplifiers are entirely controlled by the new software so that all monochromator settings can be synchronized with the data acquisition enabling programmed scans with alternating parameter sets. This versatile concept also enables the user to react immediately to changes in the sample during *in situ* studies. An interface to a three-axis stepper motor control unit is additionally included to control a sample stage which can again be synchronized with the data acquisition. Thus, spatially resolved scans and the usage of scan tools for sample alignment are feasible with the new system. Typical examples to demonstrate the features of the new data acquisition system are presented, the designed graphical user interface is described in detail and, furthermore, the crucial design parameters of a typical QEXAFS set-up are discussed.

## 1. Introduction

In the last two decades the quick-scanning extended X-ray fine structure (QEXAFS) technique (Frahm, 1988, 1989) has proven to be an invaluable tool for time-resolved *in situ* investigations of materials on the atomic scale. In the most recent QEXAFS set-ups the polychromatic beam from a bending magnet or an insertion device at a synchrotron radiation source is monochromated by a continuously oscillating channel-cut crystal before the beam passes the sample. With this approach time-resolved absorption spectroscopy at the absorption edge of a selected element is possible. Owing to its sensitivity to the short-range order it is well suited for disordered systems like liquids and nano-sized particles as relevant in many chemical and especially catalytic applications (Stötzel *et al.*, 2010a; Grunwaldt *et al.*, 2009; Singh *et al.*, 2010; Reimann *et al.*, 2011). The time resolution in the subsecond time regime is suitable for studying fast oxidation, decomposition or phase transition processes (Stötzel *et al.*, 2009a). Even surface formation or reactions on surfaces can be studied by using a grazing-incidence geometry or reflection

mode (Frahm *et al.*, 1991). Recently, several QEXAFS stations have evolved all around the world, which clearly demonstrate the scientific significance of this technique in the fields of solid state physics and chemistry (Frahm *et al.*, 2010; Khalid *et al.*, 2010; Uruqa *et al.*, 2007).

Although it is obvious from the mentioned examples that excellent scientific results can be achieved using QEXAFS, there are still two major issues where new approaches have to be found to make this technique more user-friendly and to give easier access to the growing number of users from different scientific disciplines. One of these issues is the data acquisition system (DAS), which has to meet a lot of different demands concerning the performance as well as handling and flexibility, as will be discussed in detail in this contribution. The second issue is the automated data processing which will be the topic of a forthcoming publication.

The most important property of a QEXAFS DAS is the capability to acquire, store and visualize the huge amounts of raw data that are typically generated during fast-scanning QEXAFS measurements. Recently developed QEXAFS monochromators enable scan rates of up to about 20–80

spectra per second, each one covering typically a 1 keV energy range. Usually three ionization chambers connected to V/A current amplifiers and an encoder interface to measure the Bragg angle during the crystal oscillations (Stötzel *et al.*, 2008) have to be read out simultaneously. With 16-bit resolution for the chamber signals and 32-bit values for the angular encoder values, transfer rates of about 0.2–0.8 Mbytes s<sup>-1</sup> have to be considered as the lowest reasonable data transfer rates for QEXAFS measurements in the subsecond time regime to obtain at least 1000 data points for each spectrum. In this way, files sizing hundreds of megabytes are generated within a few minutes of measuring time, while the resulting files are even about one magnitude larger if stored in the more convenient ASCII format featuring the advantage that no additional conversion is required for the subsequent data analysis. The generated data have to be acquired continuously over several hours, because prior to a new experiment it is not always obvious at which instant of time something changes in the sample, or whether a process finishes within a few milliseconds or within some hours. Furthermore, the DAS has to be flexible enough to include additional data sources, so that the user can record temperatures, electrical resistances, mass spectrometric data, *etc.* simultaneously with the QEXAFS spectra.

In all time-resolved techniques the data quality is a critical issue since a high time resolution corresponds to low statistics owing to the significantly reduced integration times for the detector signals. For several reasons the data quality is an even more challenging issue when using the QEXAFS technique. Since spectra are typically acquired within the millisecond time regime, 50 Hz (or 60 Hz) noise resulting from power supplies cannot be filtered out without affecting the measured absorption data. In a typical QEXAFS set-up noise sources are given by (i) the ground signal at the synchrotron radiation facility which might be affected by high-frequency noise owing to the connected storage-ring devices such as HF cavities and/or primary accelerator devices, (ii) ground connections with slightly different potentials leading to ground loops, (iii) environmental electrical fields in combination with insufficiently shielded detectors or poorly shielded and/or long cables, (iv) vibrations of the sample or the ionization chambers, (v) pressure changes in the ionization chambers by the gas supply and induced charges on the chamber plates by means of sound (Müller *et al.*, 2011) and (vi) the power connection and electronics of the high-voltage supplies, the current amplifiers and the data acquisition board. All these noise sources have to be considered and checked carefully when designing a QEXAFS set-up and possibly prior to each experiment. In this context a reliable data acquisition system is essential to analyze and finally to optimize the other components of the QEXAFS DAS.

In parallel to the high data rates and a sufficient data quality it is a decisive feature to display at least one spectrum every second to make sure that everything works properly during the experiment and, for example, no saturation limit of the current amplifiers, especially in the transmission signal, is exceeded. The visualization is also very helpful in the preparation of the experiment to optimize the beamline optics,

the gains and filter rise times of the current amplifiers, the gas mixtures in the ionization chambers, the sample thickness and additional parameters to obtain an adequate data quality for a meaningful EXAFS analysis (see, for example, Koningsberger & Prins, 1988).

Access to all experimental parameters in the data acquisition software is a decisive feature as well for new applications and more convenience. The monochromator motors, current amplifiers and a sample stage in combination with the data acquisition enable the user to exactly align samples, to perform scans while changing the sample position, for example, in order to check their homogeneity, to program scans measuring different edges with different time resolutions and different energy ranges (Stötzel *et al.*, 2010*b*) and to automatically document all these settings for each measurement.

## 2. Design of the data acquisition system

### 2.1. Hardware components

The entire representative QEXAFS set-up is shown in Fig. 1. The set-up is organized in such a way that all decisive devices, such as the monochromator motors, the current amplifiers, the data acquisition board and the sample stage are controlled by a single PC and also fast data acquisition as required in QEXAFS measurements is possible. A graphical user interface (GUI) provides access to all functions *via* Microsoft Visual C# software. The software is designed for Windows-operated computer systems which have proven to be very stable during measurements. The best performance can be achieved owing to the availability of the newest drivers for all hardware components for this platform. No special computer hardware is required since all devices are connected *via* USB or serial COM ports, so that it is easy to transfer the software to a new computer and to replace the PC in cases of malfunctions. The cable length limitations using USB and COM ports can be overcome by either installing the PC hardware inside the experimental hutch and enabling control *via* remote desktop or by using a COM port hub controlled *via* Ethernet and active USB extensions for connecting the USB hardware. While the application of an external ADC is also preferable in the sense of noise considerations, the data acquisition software can even run on a laptop so that the DAS can be used in a very flexible way. However, at least two displays should be available to ensure a convenient operation of the software. Many different sources have to be scanned simultaneously with the data acquisition board, *i.e.* the signal of the ionization chambers processed by the current amplifiers, the signal of the angular encoder inside the QEXAFS monochromator and eventually additional sources like temperature sensors or mass spectrometers. In addition, external trigger signals can be recorded and processed; for example, to start a new measurement when the motor control unit in tomography applications indicates that the sample position has changed. The multifunctional Keithley KUSB-3116 board was chosen here because it enables measurements

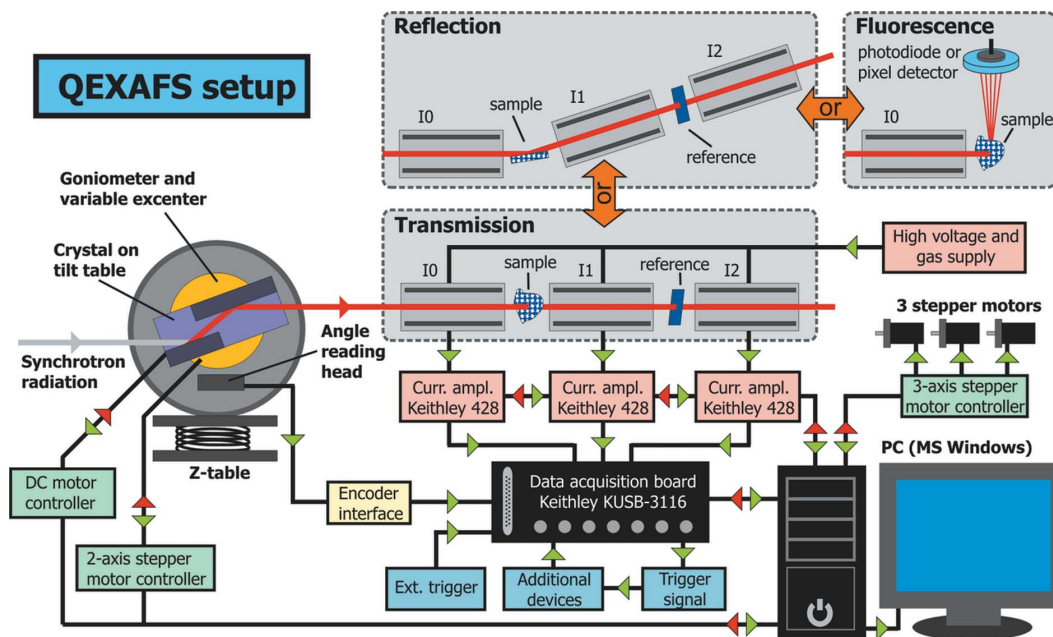


**Figure 1**  
Schematic overview of a representative QEXAFS set-up including links and directions of communication between the components.

of analogue and counter inputs in a synchronized way with high sampling frequencies, while also including trigger inputs. Additionally, the USB connection of the board allows a flexible and mobile application. Data acquisition is performed *via* a multiplexer with up to 500000 16-bit values per second, which is sufficient for the requirements specified above. With a typical EXAFS transmission set-up consisting of three ionization chambers which occupy three channels of the board, and the angular encoder (which occupies another two 16-bit channels since totally 32-bit integer values are acquired), all in all each data point is build up out of five 16-bit channels. Thus a maximum of 100000 complete data points per second is achievable with the present set-up. Owing to the acquisition steps of the multiplexer determined by the sampling frequency, a time shift between the individual values of each data point occurs. This time shift can be corrected *via* a spline interpolation or reduced to a negligible level by sufficient oversampling. The data acquisition board can also be used to control the experiment *via* the included trigger functions and/or digital TTL outputs.

The connected three-axis stepper motor controller can drive stepper motors with micro-stepping resolution, thus very accurate positioning is possible. The monochromator hardware consists of a channel-cut crystal which can be oscillated at up to 40 Hz resulting in 80 spectra  $s^{-1}$  since one full oscillation includes one spectrum measured with increasing and one with decreasing energy. Furthermore, two stepper motors are used to adjust the variable excentric and to rotate the whole oscillating tilt-table mechanics. The excentricity defines the amplitude of the crystal oscillation and thus the energy window covered by the scan. The rotation of the whole tilt-table construction is necessary to move this energy window to the absorption edge of interest. To change, for example, from

an XANES range to a full EXAFS scan the excentricity has to be enlarged, but the resulting energy window has also to be shifted to higher energies. Otherwise, both post- and pre-edge regions would be extended simultaneously, which is not favorable. An angular encoder records the oscillations with a resolution of 0.03 arcsec synchronized to the signals of the ionization chambers which are used to record the absorption spectra. These components are described in detail in previous publications (Stötzel *et al.*, 2008, 2010b; Frahm *et al.*, 2005).

## 2.2. Software design

The main GUI of the data acquisition software is shown in Fig. 2. All settings are comfortably accessible directly or indirectly *via* the five sub-GUIs: 'Monochromator Motors', 'Current Amplifiers', 'Sample Stage', 'Extra Plotter' and 'Binary to ASCII'.

**2.2.1. The main GUI.** From the main GUI it is possible to start and stop QEXAFS scans. After selecting the data acquisition board, setting up plotting and acquisition parameters, selecting an output file for the next measurement and choosing one of the acquisition modes described below, the user can start a scan instantaneously, while an accompanying information file documents all settings. Storing the data to the hard disc is organized in buffers which are part of the libraries included in the driver software of the board. The number and size of buffers as well as the sampling frequency have to be adjusted by the user prior to each measurement since these parameters are decisive in defining the data density and enabling the continuous data acquisition. If the first buffer is completely filled with data the next empty buffer in the waiting list immediately starts to receive data. At the same time the data of the first buffer is written to the hard disc and

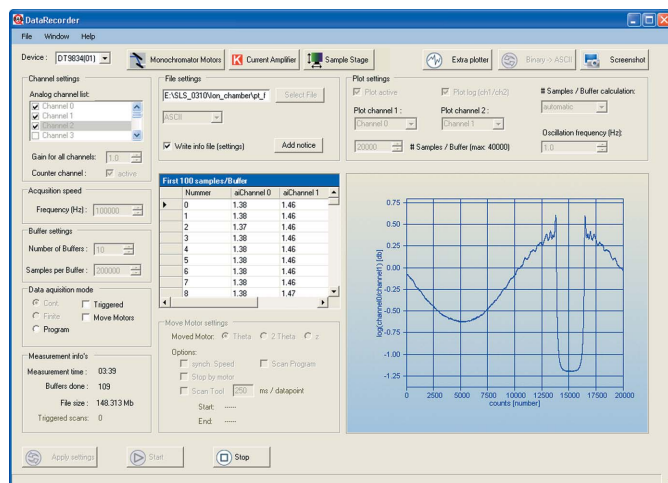


**Figure 2** Main GUI of the data acquisition software during data acquisition.

sent to the plot windows. In the case of continuous measurements empty buffers can be filled again and the size of the buffers has only to be chosen large enough to enable continuous data storage on hard disc without conflicts. In the case of finite measurements which automatically stop after a while the number and size of the buffers determine the acquisition time. Stable data acquisition over many hours is, for example, possible with buffers which are filled within 1 or 2 s and this is also a reasonable refresh rate for the plot window. The plot window can display at least half of the data from each buffer which is plotted *versus* the position in the buffer which corresponds to units of acquisition time.

Finite and continuous scans are the two basic acquisition modes for QEXAFS measurements and can also be combined with the trigger input of the acquisition board. In the case of continuous measurements only one trigger signal is expected to start the acquisition which has to be stopped manually by the user. In the case of finite acquisition mode the trigger starts a finite measurement according to the chosen buffer settings. Afterwards, the DAS waits for the next trigger signal which again starts a new finite scan while the data are written to a new file. This operation proceeds with consecutively numbered files until it is aborted by the user.

The 'Move Motors' option initializes the communication to the three-axis stepper motor control unit for the sample stage. In this case the user can select a motor for which the start and end positions are imported directly from the 'Sample Stage' GUI. Now, a scan can be started so that the DAS starts to acquire data (eventually waiting for a trigger signal) and to move the selected motor at the same time. The data acquisition stops as soon as either the motor reaches the final position or the user aborts the scan. In most sample alignment applications only one channel has to be recorded with a relative low sampling frequency. This is possible with the 'Scan Tool', which provides a maximum of four data points per second. Since these scans are not organized in buffers, the signal of the selected channel is plotted live *versus* the position of the selected motor and it is possible to save the data in a separate

file afterwards. Furthermore, a 'Scan Program' function is implemented to acquire data consecutively at different predefined motor positions as set up in the 'Sample Stage' GUI. This works in principle as described for the triggered finite measurements, with the difference that now a new measurement is not externally triggered but internally as soon as the next motor position is reached.

Complementary to the already described continuous and finite measurement modes it is possible to choose 'Program' as a third option. In this case communication with the 'Monochromator Motors' GUI is initialized and it is possible to define parameter sets for scans as described in the corresponding section below.

With the plotting settings a single channel can be plotted *versus* time or, for example, the logarithm of a quotient of two channels yielding the desired absorption spectra. Additionally, the number of plotted samples from each buffer can be varied up to a maximum of 50% of the total number of samples per buffer. Particularly during experiments measured with 1 Hz or faster it is not possible to check each single spectrum during the experiment. However, it is essential to observe the spectra of one crystal oscillation period every one or two seconds in order to check the acquired data and to follow the course of the investigated reaction. Thus, an automatic samples per buffer calculator can be activated which always plots only one oscillation out of each completed buffer. All plot options can be modified comfortably also during the measurement, while up to three additional plot windows can be opened to plot several signals at the same time. This is especially helpful when setting up the experiment to see how the beamline components (slits, mirrors, insertion device, *etc.*) and detector settings (gas and high voltage for ionization chambers, amplifier gains, filters, *etc.*) affect the resulting signals and also during the experiment to check whether saturation limits are reached owing to changes of the sample absorption. Furthermore, it is also possible to plot the data of the angular encoder which is measuring the crystal oscillation and can be used to check the monochromator mechanics.

**2.2.2. Monochromator motors.** The 'Monochromator Motors' GUI as shown in Fig. 3 gives access to all motors of

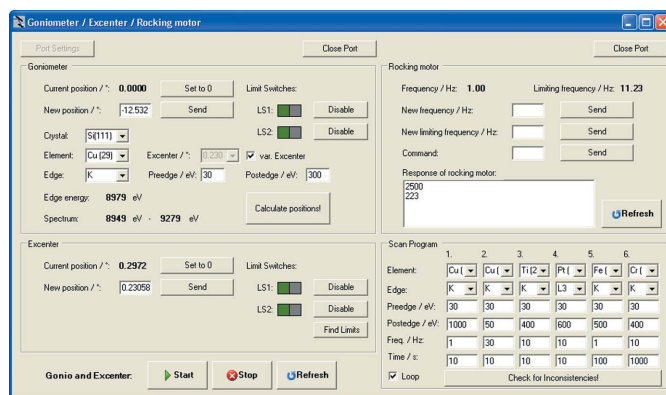


**Figure 3** GUI to control the mean Bragg angle, the Bragg angle range and the crystal oscillation frequency.

the QEXAFS monochromator. These motors are the ‘Goniometer’ used to adjust the central Bragg angle corresponding to the mean energy value of the spectrum, the ‘Rocking motor’ causing the crystal oscillation yielding the time resolution and the ‘Excenter’ which determines the amplitude of the crystal oscillation and thus the energy range of the spectrum. The mechanics are described in detail elsewhere (Stötzel *et al.*, 2010*b*). Communication to the motors is established *via* RS232 to an additional external two-axis stepper motor controller (miCos GmbH) for the goniometer/excenter motors and a DC motor controller (Faulhaber GmbH) for the rocking motor. The software controls for the rocking motor allow adjustment of the frequency of the motor and setting of a maximal frequency. If further adjustments of the controller are necessary, commands can be sent manually, while a text box documents all responses of the controller. The goniometer and excenter can be moved independently or synchronized at the same time. For these motors it is also possible to enable or disable limit switches which can be used for safety reasons and/or as calibration points since no additional encoders are used to monitor the position of these motors. This is sufficient owing to the huge accuracy and reliability of the movements.

To enhance the convenience an additional Bragg equation calculator is included in the ‘Goniometer’ section. Here it is possible to select the monochromator crystal, the absorption edge of interest and the desired energy interval and to let the program calculate the corresponding goniometer and excenter settings. The energy values for the absorption edges are taken from the literature (Bearden & Burr, 1967).

In addition to the motor controls it is possible to define multiple parameter sets in the ‘Scan Program’ section. These can be scanned with only one file for each parameter set or in a repetitive mode with consecutively numbered files. Typically, a new scan starts as soon as all motors have reached their final positions of the actual parameter set, but data can also be stored in a single file, where the regions with moving motors are also included in the measurement. Furthermore, it is possible to define the acquisition time individually for each parameter set.

**2.2.3. Current amplifiers.** The application of Keithley 428 current amplifiers has proven to be a good choice for QEXAFS measurements because these current amplifiers are very fast, reliable and they feature a high signal-to-noise ratio. The GUI to control the current amplifiers is shown in Fig. 4. The connection is established *via* GPIB using a USB-GPIB interface which is initialized as soon as the GUI is loaded. The connected amplifiers are selected *via* their GPIB addresses. Their settings such as, for example, gain and filter rise time are displayed and can be changed individually. The filters can also be switched on and off or the ‘Auto Filter’ function of the amplifiers can be activated. Furthermore, the ‘Zero Correct’ function can be used to calibrate the amplifiers, while the activation of the ‘Zero Check’ option leads to a stable 0 V output from the current amplifiers which can be used for manual zero correction and for checking noise on the ADC inputs. The ‘Gain  $\times 10$ ’ function extends the amplification by one order of magnitude.

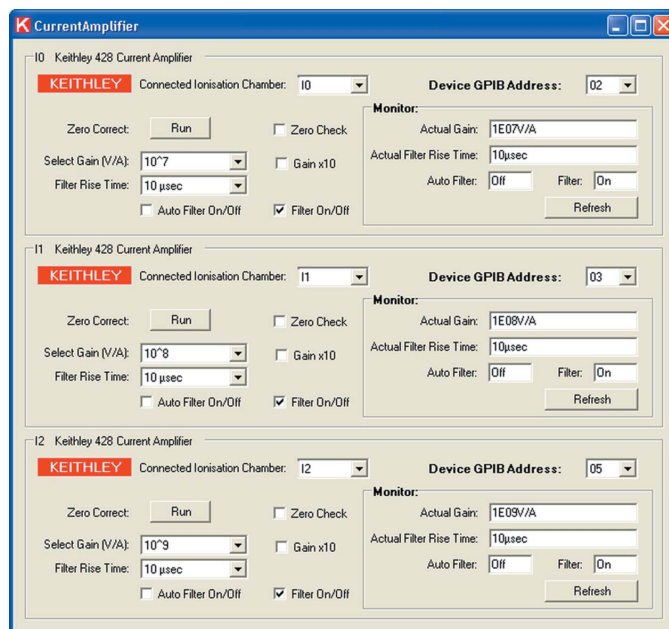


**Figure 4**  
GUI to control the current amplifiers connected to the ionization chambers.

**2.2.4. Experimental stage.** Controlling the sample position is enabled by the application of a three-axis stepper motor control unit with micro-stepping function (Trinamics GmbH). The controller is accessible *via* an additional GUI as shown in Fig. 5. Each stepper motor can be tuned in current, standby current, speed and backlash. It is possible to store and retrieve all motor parameters and to convert the motor position from micro-step numbers to comfortable units. The GUI was consciously kept simple to give direct access only to the most important motor controller settings. Each motor can be moved to an absolute position or relative to the actual position and also several motors can be moved simultaneously. Furthermore, it is possible to synchronize the speed of two motors, so that both reach their final positions at the same time. These options were implemented to allow, for example,  $\theta$ - $2\theta$  reflec-

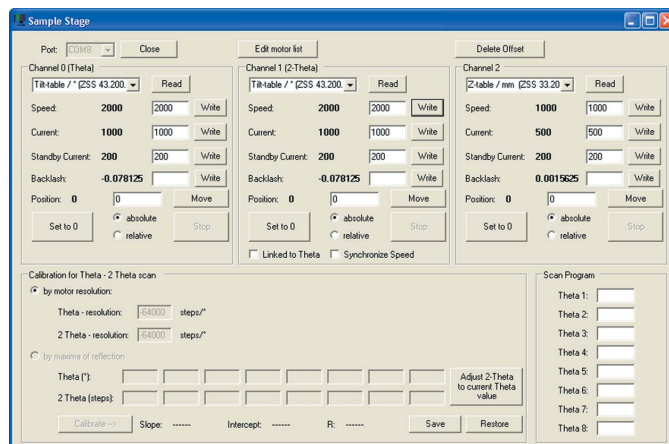


**Figure 5**  
GUI to control the three-axis stepper motor control applicable for sample stage purposes.

tivity scans to be performed. Additionally, eight  $\theta$  values can be set up for a scan program which is started from the main GUI as described in the corresponding paragraph.

### 3. Experimental verification

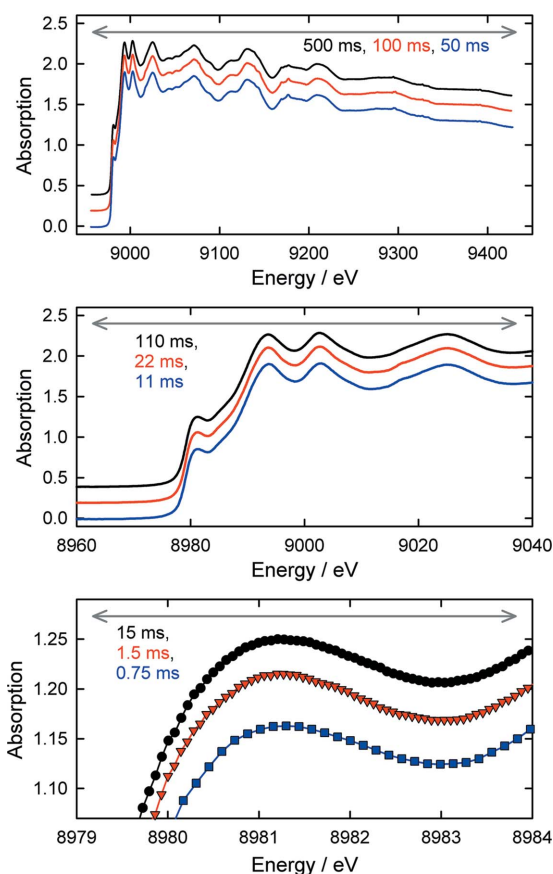
Published scientific investigations have proven the capability of the presented set-up for QEXAFS experiments (Stötzel *et al.*, 2008, 2009a,b, 2010a,b; Grunwaldt *et al.*, 2009; Singh *et al.*, 2010; Reimann *et al.*, 2011; Zhou *et al.*, 2010). A detailed view on specific aspects of the performance of the described DAS system is presented in the following. All EXAFS data were acquired with the stationary QEXAFS monochromator at the SuperXAS beamline at the Swiss Light Source (Frahm *et al.*, 2010).

#### 3.1. Data acquisition speed

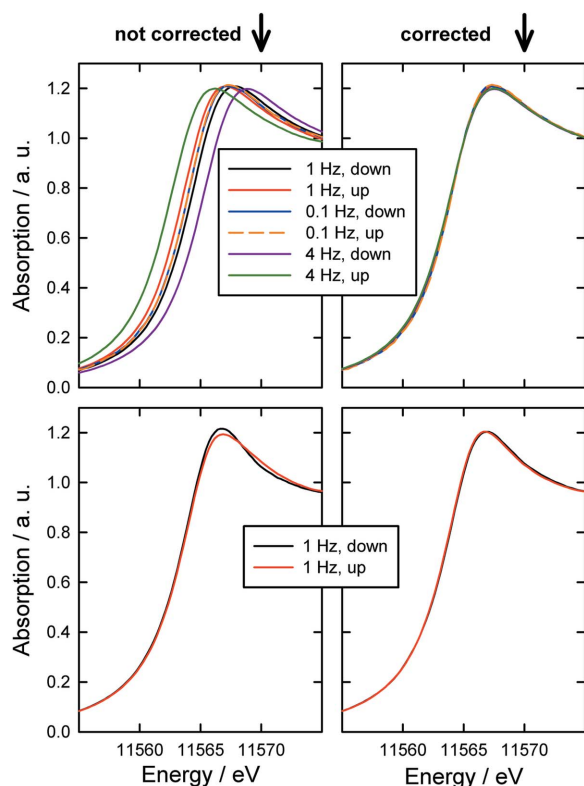
In Fig. 6 single depicted absorption spectra of a Cu metal foil at the Cu *K*-edge acquired with different scan speeds are shown as well as enlarged intervals. The spectra cover an energy interval of almost 500 eV and were measured with 1, 5 and 10 Hz crystal oscillation frequency which is equivalent to a time resolution of one spectrum each 500, 100 and 50 ms, respectively. A frequency of 1 Hz corresponds to one full oscillation of the monochromator crystal in 1 s, so that two

spectra, one with increasing and one with decreasing energy, are scanned within this period. Minor details of the Cu *K*-edge are clearly resolvable even in the spectra with the best time resolution. The interval of 5 eV measured within 0.75 ms still consists of plenty of data points considering a typical energy resolution of about 1 eV which is determined by the beamline optics and the Si(111) monochromator crystal. The high data density in energy is very important for further data treatment since it enables averaging not only over several data points within a single spectrum but also over several consecutive spectra without introducing jitter errors. Averaging over several spectra is a very useful and powerful tool in QEXAFS data processing and is facilitated by the installation of the high-resolution angular encoder system. In this context it has to be considered that it is not possible to predefine the individual energy values of the acquired spectra, and thus each spectrum consists of values recorded at slightly different energy values. With a reasonable data point density as shown in Fig. 6 it is possible to interpolate the spectra on a uniform energy grid and then to average over several spectra. An example for the benefit of this variable averaging of QEXAFS spectra is given by Reimann *et al.* (2011). From Fig. 6 it is also obvious that a time shift between the values of each data point owing to the multiplexed acquisition mode is not relevant with a sufficient data density owing to oversampling.

The acquisition of angular encoder data and the data generated by the ionization chambers is perfectly synchronized. Nevertheless, owing to the finite response time of the detector system, the signal of the ionization chambers is slightly delayed in the raw data with respect to the immediate signal of the encoder. This time delay is constant if all parameters of the detector system remain unchanged. It manifests itself as an apparent energy shift between the spectra measured in the up and down directions. It also leads to an apparently increasing energy separation of those spectra, if the frequency of the crystal oscillation is increased. This time delay typically amounts to few hundred microseconds and is not caused by the monochromator mechanics or the data acquisition hardware. The effects on the spectra are shown in Fig. 7 where averaged spectra of a Pt-containing sample at the Pt *L*<sub>3</sub>-edge are shown. The sample was placed between the first two ionization chambers. An additional Pt metal foil was mounted between the second ionization chamber and a Si photodiode used as a detector for the transmitted intensity. Such a detector exhibits a significantly faster time response than ion chambers, and thus the raw signal of the photodiode does not show the apparent energy shift mentioned above between both spectra. The spectrum of the reference Pt metal foil was used to calibrate the edge energy. It can be seen in Fig. 7 that owing to the different time responses of ionization chambers and the Si diode the resulting spectra of the sample are separated in energy by an amount depending on the scan direction and the scan speed. If the signals of the chambers are shifted backwards in time during data analysis by 250  $\mu$ s to match the response time of the Si diode, the spectra are perfectly congruent after calibrating the energy with the Pt foil. In Fig. 7 the spectra of the reference foil are also shown,



**Figure 6** Spectra of a Cu metal foil at the Cu *K*-edge measured with different time resolutions. Different regions of the same measurement are shown.

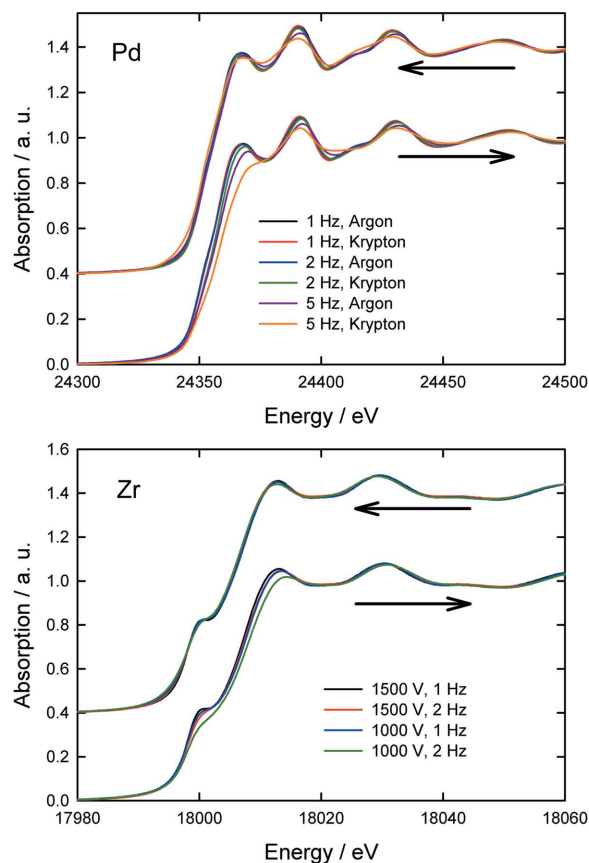

**Figure 7**

Normalized absorption spectra in both scan directions of a Pt-containing sample measured with two ionization chambers (top) and a Pt metal foil as reference between the second chamber and an additional Si diode (bottom). The spectra were calibrated in energy *via* the Pt metal foil spectra. Additionally, the same spectra with a time correction applied to the ion chamber signals are shown.

and small differences show up in the uncorrected data. However, the spectra become indistinguishable in both scan directions if a time shift is applied to the signal of the second ionization chamber, which is the detector for the primary intensity illuminating the Pt foil. If, as in most transmission experiments, detectors with similar response times are used, this effect is hardly observable. However, if very accurate and very fast measurements are required, it is advisable to determine the time shift prior to the experiment and to correct the acquired data afterwards. Even a constant time shift in all detectors shifts the absorption spectra with respect to the encoder values as mentioned above. If detectors with different response times are used, as, for example, in fluorescence applications, this time correction is prerequisite when using subsecond time resolution to obtain highly accurate results. The use of fast detectors for all channels would eliminate the artificial shifts in the spectra directly. Photodiodes are feasible for measuring the transmitted intensity, because that detector does not need to be transparent. For the detection of the primary intensity, ionization chambers are very convenient because they are sufficiently transparent and yield decent currents, which can be easily adjusted by changing gas filling, gas pressure or length. If one intends to determine the primary intensity from, for example, scattering from thin synthetic foils using fast photodiodes as detectors, in general only weak

signals can be obtained, which impair the signal-to-noise ratio. In addition, a low signal level implies different amplifier settings and thus rise times, recreating the conditions which should be avoided. However, other detection schemes or transparent detectors such as diamond foils should be evaluated with respect to high-accuracy high-speed data acquisition.

The time response of a QEXAFS system depends not only on data acquisition speed but also on the design of the ionization chambers and their gas fillings, the applied high voltage and the current amplifiers. This has to be considered when realising a QEXAFS DAS. Fig. 8 demonstrates how the gas filling of the ionization chambers and the applied high voltage can affect the QEXAFS spectra. The Pd metal foil was measured with exactly the same set-up except for the gas in the second ionization chamber which was changed from Ar to Kr, both at ambient pressure, while the filling of the first chamber remained Ar. The XANES spectra shown are cut out from full EXAFS spectra with a range of 1850 eV; thus the shown interval was scanned in 67.5, 33.8 and 13.5 ms (highest scan speed at this absorption edge:  $\sim 13100 \text{ eV s}^{-1}$ ). Furthermore, the spectra shown are the result of averaging over 20, 40 and 100 spectra to obtain the same statistics for each curve. With a crystal oscillation frequency of 1 Hz the gas filling does


**Figure 8**

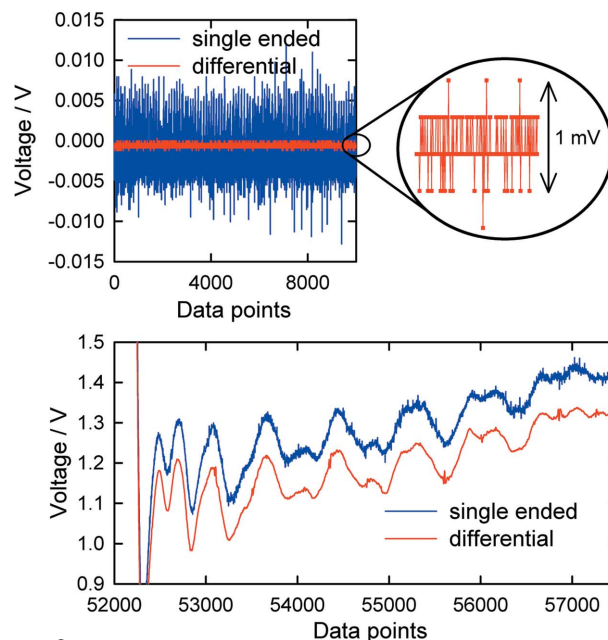
Normalized absorption spectra of a Pd metal foil at its *K*-edge with variable gas in the second ionization chamber (top) and a Zr metal foil at its *K*-edge with variable high voltage applied to the ionization chambers. The arrows show the scan direction of the plotted spectra which are shifted with respect to each other for clarity.

not have a significant influence on the observed shape of the Pd metal foil spectrum. With 2 Hz the spectrum measured with Kr deviates from the 1 Hz spectra while the 2 Hz spectrum measured with Ar is still fine. The deviations are more evident in the scan direction with increasing energy owing to the sharp features in the XANES following directly after the edge jump. This is even more evident for the case of 5 Hz. Here the spectrum measured with Ar also starts to show displacements but these are much more enhanced with Kr. This effect can be accounted to the much reduced mobility of Kr ions in the ionization chamber (Sitar *et al.*, 1993). Obviously the slow Kr ions require more time to reach the chamber plate in the ionization chamber, thus leading to artefacts in the spectra and a reduced usable measurement frequency.

The Zr metal foil in Fig. 8 was measured with 1000 V and 1500 V at the plates of the ionization chambers which are mounted at a distance of 10 mm from each other. Here the original spectra have an energy range of 980 eV resulting in scan times of 21.3 and 42.6 ms for the shown interval (highest scan speed at absorption edge:  $\sim 3400 \text{ eV s}^{-1}$ ). The spectra are the result of averaging over 20 and 40 spectra. The shoulder in the absorption edge is a good indicator showing that even at 1 Hz the resolution is decreased with only 1000 V at the chambers. At 2 Hz the differences are even more evident and demonstrate that the high voltage is preferably chosen as high as possible to increase the time resolution by increased speed of the charge carriers owing to increased electrical fields in the chambers.

### 3.2. Noise of detection system

The data acquisition board allows scanning of the analogue channels in single-ended and differential mode. In differential mode the number of usable analogue input channels is reduced from 16 to eight; however, it provides a significantly reduced noise level. This is shown in Fig. 9, where the 0 V reference signal of the current amplifier was recorded in both modes. Whereas in the single-ended measurement the values are mainly in a band of  $\pm 7 \text{ mV}$ , the noise level in the differential set-up is of the order of the resolution of the 16-bit ADC; in this case the least significant bit corresponds to 0.31 mV. Applied to real QEXAFS data it is obvious that the differential mode is the preferable choice as shown in Fig. 9, where the raw signal of the second chamber in the typical EXAFS transmission set-up is plotted. A Pt metal foil was placed right in front of the second chamber and scanned at the Pt  $L_3$ -edge. Again the noise level is much lower in differential mode and the remaining distortions can be attributed to the fact that the data are not yet normalized to the signal of the first chamber. The eight channels available in differential mode are more than sufficient for all kinds of EXAFS experiments, and the differential mode is now used as standard. Several scientific examples, where especially small changes in the absorption spectra had to be detected, demonstrate the progress possible by this measurement mode (Zhou *et al.*, 2010; Stötzel *et al.*, 2009b).

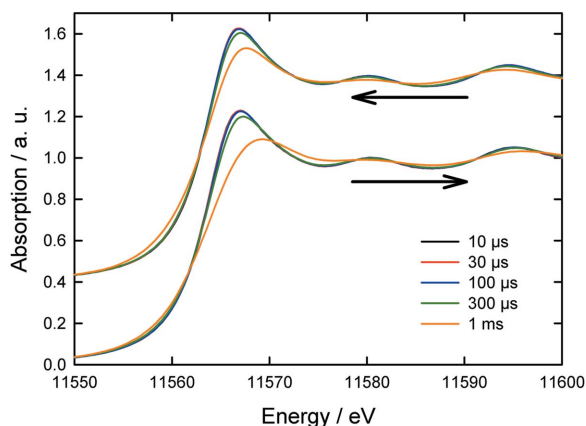


**Figure 9** Exemplary measurements in single-ended and differential mode with a 0 V reference output signal of a Keithley 428 current amplifier (top) and the signal of an ionization chamber located downstream of a Pt metal foil measuring the Pt  $L_3$ -edge without normalization to the impinging intensity (bottom).

### 3.3. Current amplifier control

The current amplifier settings are a decisive factor in optimizing QEXAFS measurements, *i.e.* the filter rise time, which determines how long the output signal of the current amplifier requires to increase from 10% to 90% of the input signal. With an adjustable rise time it is possible to filter out high-frequency noise; however, a too long rise time can also smooth out significant features of the spectrum. Many EXAFS spectra, especially those of transition metals at the  $L$ -edges, provide sharp features like an intense white-line, which is affected by high filter rise times. While this is to a certain degree negligible when only the EXAFS is analyzed, it is very important for XANES analysis, where such sharp features have a significant influence on, for example, quantitative results of linear combination fits. Many current amplifiers intrinsically have rise times which are too long for QEXAFS; even the commonly used Keithley 428 amplifiers can be the limiting factor concerning time resolution. In Fig. 10 absorption spectra of a Pt metal foil at the Pt  $L_3$ -edge measured with different filter rise times are presented. The full range of these spectra measured with 5 Hz amounted to 800 eV leading to a scan speed of about  $6000 \text{ eV s}^{-1}$  at the absorption edge. In the middle of the spectrum a maximum scan speed of about  $12500 \text{ eV s}^{-1}$  has to be considered owing to the sinusoidal movements of the crystal. Considering an energy resolution of about 1 eV which is a typical value for a Si(111) monochromator in this energy range, it is possible to calculate the required time resolution of the detector system which is in this case simply the reciprocal value of the scan speed, which amounts to about  $170 \mu\text{s}$  at the Pt  $L_3$ -edge. This is in perfect agreement with the spectra in Fig. 10 where excellent data are



**Figure 10**

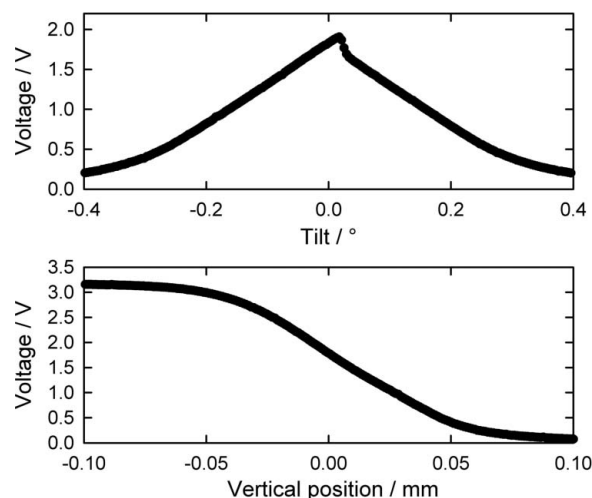
Normalized absorption spectra of a Pt metal foil at the Pt  $L_3$ -edge measured with 5 Hz crystal oscillation frequency and variable filter rise times of the current amplifiers. The arrows indicate the scan direction and the spectra are vertically shifted for clarity.

measured with a filter rise time of up to 100  $\mu\text{s}$ , while a 300  $\mu\text{s}$  rise time leads to deviations. While, as shown with this example, it is possible to calculate reasonable filter rise times for each specific experiment, it might be preferable to acquire data with the lowest achievable rise times and to filter the data by software processing subsequently. The filter rise time of the Keithley 428 current amplifiers has a lower limit of 10  $\mu\text{s}$  for gains of  $10^6$  and  $10^7$ . For  $10^8$  this limit increases to 40  $\mu\text{s}$ , for  $10^9$  to 100  $\mu\text{s}$  and for  $10^{10}$  to even 250  $\mu\text{s}$  (Keithley Instruments Inc., 1999). To measure spectra at the Pt  $L_3$ -edge with 800 eV scan range and up to 20 Hz crystal oscillation frequency, amplifications of  $10^8$  or less thus have to be used. These limitations have to be considered when preparing a QEXAFS experiment or selecting a radiation source.

The control of the current amplifiers in combination with the visualization capabilities of the DAS is very helpful for optimizing slits and mirrors of the beamline so that the resulting signals are well distributed over the dynamic range of the current amplifiers. Furthermore, the implementation of the current amplifier controls in the data acquisition system is preferable in the sense of documentation because all current amplifier settings are stored automatically to the information file which is generated simultaneously with each individual data file.

### 3.4. Three-axis stepper motor control

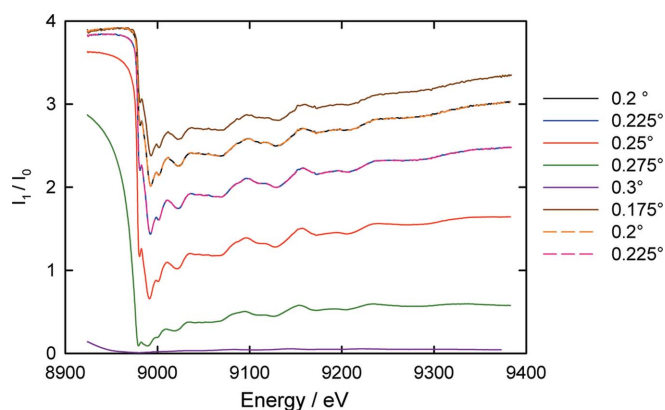
The application of the ‘Scan Tool’ software segment was tested in a reflection-mode EXAFS (RefEXAFS) experiment. For this kind of measurement the sample has to be thoroughly positioned in the beam. For this purpose rocking scans are performed, where the intensity in the detector for the reflected intensity, *i.e.* an ionization chamber filled with Ar in the present case, is measured for  $2\Theta = 0$  while the incidence angle  $\Theta$  of the sample was scanned. As recognizable in Fig. 11 an equal-sided triangle will evolve if a linear interpolation of the increasing and decreasing leg to the intersection is performed. The maximum of this triangle corresponds to the  $\Theta = 0^\circ$  position. In addition, the sample has to be scanned

**Figure 11**

Intensity in the detector downstream of the sample acquired during the alignment of a copper thin-film sample for a RefEXAFS measurement varying the incident angle (‘rocking scan’) (top) and the vertical position in the beam (bottom).

in the  $z$ -direction to locate the correct vertical position with half of the impinging intensity. To exactly align the sample for a RefEXAFS measurement these two scans have to be repeated iteratively to improve the alignment as, for example, described by Holy *et al.* (1999).

The ‘Scan Program’ function can be effectively used for RefEXAFS measurements as shown in Fig. 12, where spectra of a thin Cu layer sputtered on a glass substrate were measured under various different incident angles in reflection at the Cu  $K$ -edge. Such a variation of the incidence angle is extremely useful for layered sample systems because a variation of the incidence angle allows the variation of the penetration depth of the incident X-rays, and thereby a non-destructive depth-profiling of the sample is possible by EXAFS (Heald *et al.*, 1988; Cheong *et al.*, 2001; Keil & Lützenkirchen-Hecht, 2009). Each plotted spectrum is the

**Figure 12**

RefEXAFS spectra of a thin copper layer on glass at the Cu  $K$ -edge acquired using the ‘Scan Program’ function of the DAS for different incidence and exit angles. The presented data were acquired with 1 Hz oscillation speed (500 ms per spectrum) and the data are averaged over ten subsequent spectra. Note the high reproducibility of the scans measured for identical incidence angles.

result of averaging ten original spectra measured with 1 Hz crystal oscillation frequency (one spectrum each 500 ms). To obtain real reflection spectra several geometrical corrections as described in detail in the literature (Holy *et al.*, 1999) are necessary. Here the focus is on the capabilities of the software functions, and thus the raw ratios of the reflected ( $I_1$ ) and incident ( $I_0$ ) intensities  $I_1/I_0$  are shown in Fig. 12. The scan cycle starts with an incident angle of  $\Theta = 0.2^\circ$ , increasing stepwise by  $0.025^\circ$  up to  $0.3^\circ$  and then going down to  $0.175^\circ$  before restarting at  $0.2^\circ$  again. One cycle takes only 90 s so that such a procedure can also be used to study time-resolved processes at surfaces with depth resolution. Thus, it is not only possible to perform time-resolved studies of the structure of the surface but also the structure distribution within the thin films. Fig. 12 also demonstrates the reproducibility of the system since the spectra of the second cycle are exactly congruent with those of the first cycle.

The DAS also provides the possibility of carrying out  $\theta$ - $2\theta$  scans which can be used to analyse layer thicknesses, layer densities and surface roughnesses.

### 3.5. Monochromator control

The flexibility provided by the monochromator control functions as described in §2.2.2, namely the change of mean energy value, energy range and time resolution, is demonstrated in Fig. 13 where a Cu foil is measured with different energy ranges from 30 eV to 2700 eV while maintaining a small interval for the pre-edge region. Each spectrum shown

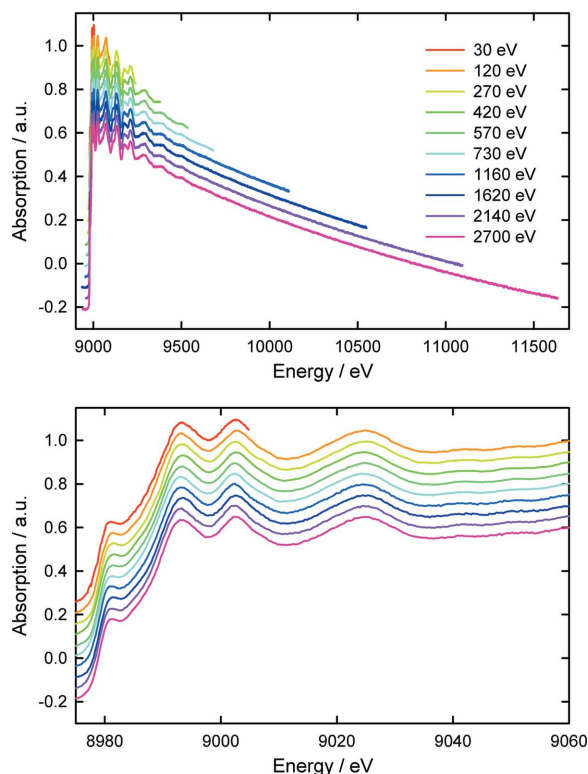


**Figure 13** Cu  $K$ -edge spectra each measured within 500 ms with different scan ranges (top) and an enlarged view on the XANES region (bottom).

is measured within only 500 ms. The largest spectrum covers a range sufficient to measure Cu EXAFS and Pt  $L_3$ -edge XANES within one spectrum with subsecond time resolution. Within a few seconds the control program allows switching to a shorter range covering only the Cu EXAFS or even only the XANES region, while the same energy ranges can be adjusted, for example, at the Pt  $L_3$ -edge. Even scans with alternating parameter sets can be performed if, for example, two edges are too far apart in energy to be covered by one scan. With the presented set-up it is possible to synchronize the spectrum settings with, for example, programmable mass flow controllers or sample heaters and react to structural changes in the sample which gives rise to completely new applications of the QEXAFS technique. Further experimental data demonstrating the mechanical versatility and stability of the monochromator system are given by Stötzel *et al.* (2010b).

### 4. Conclusions

The data acquisition system for a QEXAFS set-up aiming at acquiring spectra in the millisecond regime has been described in detail. Fast data acquisition with at least 100000 data points each second is essential for EXAFS spectra with repetition rates of the order of 10 Hz to exploit the full energy resolution and also to enable, for example, averaging over multiple spectra. Moreover, the continuous data acquisition exhibits a very low noise level. There are no observable dead-times, and thus physical and/or chemical processes can be investigated without interruptions, even if these are monitored for several hours. An intuitive and user-friendly GUI was designed to give easy access to the various features of the software of the DAS. The visualization of the acquired data is a key feature for optimizing the preparation of each measurement concerning the adjustment of beamline optics, detector system and sample alignment, as well as for monitoring changes in the ongoing measurement for a preliminary data analysis or for observing structural changes in real time. We further discussed critical issues in the QEXAFS DAS with respect to ionization chambers and current amplifiers. It has been shown that new hardware developments concerning the ionization chambers and the current amplifiers are important to further increase the time resolution of the QEXAFS technique.

Besides the fast data acquisition, full control of monochromator, current amplifiers and additional stepper motors is additionally included in the new software resulting in a complete platform with all functions that are required for QEXAFS experiments. This very flexible system is usable with any commercially available desktop or laptop PC. It is possible to synchronize the data acquisition with the sample alignment as well as the monochromator controls, which paves the way for plenty of interesting applications in, for example, catalysis and surface physics. Since the software is not at a limit yet, the control of other hardware components such as, for example, a gas control system for the ionization chambers can be included.

Concerning the acquisition speed, the next step is to evaluate recently developed data acquisition boards which allow

measurement of several even faster channels simultaneously using several individual analogue-to-digital converters (ADCs) in parallel instead of a single ADC and a multiplexer. This is the favourable way to collect the data, since in this case the channels are completely independent of each other and no corrections have to be applied to correct the time shift between the channels. However, it has to be verified whether a similar high data quality as presented in this paper is achievable.

We acknowledge the Swiss Light Source for beam time and M. Nachttegaal for his excellent support at the SuperXAS beamline. Further we are indebted to Christian Rolf and Jan Gasse for their coding work which was essential for the software development process.

## References

- Bearden, J. A. & Burr, A. F. (1967). *Rev. Mod. Phys.* **39**, 125–142.
- Cheong, S., Bunker, B., Hall, D. C., Snider, G. L. & Barrios, P. J. (2001). *J. Synchrotron Rad.* **8**, 824–826.
- Frahm, R. (1988). *Nucl. Instrum. Methods Phys. Res. A*, **270**, 578–581.
- Frahm, R. (1989). *Rev. Sci. Instrum.* **60**, 2515–2518.
- Frahm, R., Barbee, T. W. Jr & Warburton, W. (1991). *Phys. Rev. B*, **44**, 2822–2825.
- Frahm, R., Nachttegaal, M., Stötzel, J., Harfouche, M., van Bokhoven, J. A. & Grunwaldt, J.-D. (2010). *AIP Conf. Proc.* **1234**, 251–255.
- Frahm, R., Richwin, M. & Lützenkirchen-Hecht, D. (2005). *Phys. Scr.* **T115**, 974–976.
- Grunwaldt, J. D., Beier, M., Kimmerle, B., Baiker, A., Nachttegaal, M., Griesebock, B., Lützenkirchen-Hecht, D., Stötzel, J. & Frahm, R. (2009). *Phys. Chem. Chem. Phys.* **11**, 8779–8789.
- Heald, S. M., Chen, H. & Tranquada, J. M. (1988). *Phys. Rev. B*, **38**, 1016–1026.
- Holy, V., Pietsch, U. & Baumbach, T. (1999). *High-Resolution X-ray Scattering from Thin Films and Multilayers*, Springer Tracts Modern Physics, Vol. 149, pp. 1–251. Berlin: Springer.
- Keil, P. & Lützenkirchen-Hecht, D. (2009). *J. Synchrotron Rad.* **16**, 443–454.
- Keithley Instruments Inc. (1999). *Model 428 Current Amplifier Instruction Manual*. Cleveland: Fourth Printing.
- Khalid, S., Caliebe, W., Siddons, P., So, I., Clay, B., Lenhard, T., Hanson, J., Wang, Q., Frenkel, A. I., Marinkovic, N., Hould, N., Ginder-Vogel, M., Landrot, G. L., Sparks, D. L. & Ganjoo, A. (2010). *Rev. Sci. Instrum.* **81**, 015105.
- Koningsberger, D. C. & Prins, R. (1988). *X-ray Absorption*. New York: Wiley.
- Müller, O. *et al.* (2011). In preparation.
- Reimann, S., Stötzel, J., Frahm, R., Kleist, W., Grunwaldt, J.-D. & Baiker, A. (2011). *J. Am. Chem. Soc.* Submitted.
- Singh, J., Nachttegaal, M., Alayon, E. M. C., Stötzel, J. & van Bokhoven, J. A. (2010). *ChemCatChem*, **2**, 653–657.
- Sitar, B., Merson, G. I., Chechin, V. A. & Budagov, Y. A. (1993). *Ionization Measurements in High Energy Physics*, Springer Tracts in Modern Physics, Vol. 124. Berlin: Springer.
- Stötzel, J., Lützenkirchen-Hecht, D., Fonda, E., De Oliveira, N., Briois, V. & Frahm, R. (2008). *Rev. Sci. Instrum.* **79**, 083107.
- Stötzel, J., Lützenkirchen-Hecht, D. & Frahm, R. (2010*b*). *Rev. Sci. Instrum.* **81**, 073109.
- Stötzel, J., Lützenkirchen-Hecht, D., Frahm, R., Kimmerle, B., Baiker, A., Nachttegaal, M., Beier, M. J. & Grunwaldt, J.-D. (2009*a*). *J. Phys. Conf. Ser.* **190**, 012153.
- Stötzel, J., Lützenkirchen-Hecht, D., Frahm, R., Kimmerle, B., Baiker, A., Nachttegaal, M., Beier, M. J. & Grunwaldt, J.-D. (2009*b*). *J. Phys. Conf. Ser.* **190**, 012162.
- Stötzel, J., Lützenkirchen-Hecht, D., Frahm, R., Santilli, C. V., Pulcinelli, S. H., Kaminski, R., Fonda, E., Villain, F. & Briois, V. (2010*a*). *J. Phys. Chem. C*, **114**, 6228–6236.
- Uruga, T., Tanida, H., Inoue, K., Yamazaki, H. & Irie, T. (2007). *AIP Conf. Proc.* **882**, 914–916.
- Zhou, Y., Grunwaldt, J. D., Krumeich, F., Zheng, K., Chen, G., Stötzel, J., Frahm, R. & Patzke, G. R. (2010). *Small*, **6**, 1173–1179.